Influence of confinement by transverse reinforcement on the nonlinear behaviour of reinforced concrete structures

Adnane Ourabah[a], *Youcef* Bouafia[b],
Abdelkader Iddir[c], *Mohand Said* Kachi[d]

University Mouloud Mammeri,
Civil Engineering Department, L2MSGC Laboratory,
Tizi Ouzou, People's Democratic Republic of Algeria

[a] e-mail: adnane.ourabah@ummto.dz, **corresponding author,**
 ORCID iD: https://orcid.org/0009-0003-2094-8990

[b] e-mail: youcef.bouafia2012@yahoo.com,
 ORCID iD: https://orcid.org/0000-0002-4222-2176

[c] e-mail: abdelkader.iddir@ummto.dz,
 ORCID iD: https://orcid.org/0009-0006-7693-5197

[d] e-mail: kachi_ms@yahoo.fr,
 ORCID iD: https://orcid.org/0000-0001-7357-0424

Abstract:

Introduction/purpose: Structural design and calculation are based on the behavior of concrete and steel separately, without taking into account the contribution of stirrups in concrete confinement. The influence of confinement in structural modeling can be used to better approximate real behavior. The purpose of this study is to develop and validate a non-linear model for the behavior of reinforced concrete structures, taking into account concrete confinement.

Methods: A 3D finite element model is used to analyze framed structures. This model takes into account shear deformations. The cross-section of the beam is discretized into trapezoidal layers, while each layer is assumed to be uniaxially stressed. Non-linear constitutive laws are applied to the materials. For concrete confinement, the material's ductility is considered using the relationships proposed by Bouafia et al. These models are implemented in a computer program. The software monitors the behavior of column-beam structures under variable loads until reaching their load-bearing capacity.

Results: The results are compared with experiment results, focusing on maximum strength and deformability. The comparison shows very satisfactory results. In addition, the use of transverse reinforcement for

concrete confinement significantly impacts the global behavior of reinforced concrete structures by influencing the contribution of ductility.

Conclusion: The consideration of confinement in structures provides the best possible approach to the real behavior of structures. In contrast to existing calculation codes, concrete behavior laws do not take into account the contribution of confinement by transverse reinforcement.

Keywords: reinforcement, confinement, modelling, simulation, ductility, stirrups.

Introduction

In the field of engineering, particularly in construction of civil and industrial structures, design and modeling are mainly based on the finite element method (FEM). This method has developed considerably (Zienkiewicz & Taylor, 2005), initially employing a linear approach for discretizing beam elements before evolution towards non-linear methodologies (Bathe, 2006). Successive research has continued to refine and develop these approaches (Bratina et al, 2004; Rozman & Fajfar, 2009; Eltoft & Lande, 2015).

Recent models have introduced various approaches to taking non-linearity into account in the analysis of reinforced concrete structures, including concentrated non-linearities at end nodes, based on the concept of plastic hinges (Spacone et al, 1996) or distributed along the element (Spacone et al, 1992). These models aim to provide a more accurate representation of actual structural behavior, particularly in the case of complex or elongated structures subjected to high loads (Scott et al, 1982; Mander et al, 1988). Analysis of these structures requires consideration of the actual behavior of the materials used - concrete and steel - with recent studies proposing various behavioral relationships for these materials (Popovics, 1973; Bentz & Collins, 2000; Elwood & Moehle, 2003).

The main objective is to simulate the actual behavior of structures up to failure. This requires the consideration of mechanical non-linearities between stress and strain and the effects of transverse reinforcements, which not only absorb shear forces but also improve the compressive strength of concrete through a confinement effect. Recent experimental and theoretical studies have focused on the strength and ductility of ordinary concrete elements reinforced with transverse reinforcement, illustrating the significant impact of confinement on the behavior of concrete sections, whether circular or rectangular (Blume et al, 1961; Roy & Sozen, 1965; Soliman & Yu, 1967).

Several recent experimental and theoretical studies have analyzed the strength and ductility of ordinary concrete elements reinforced with transverse steel. This research has highlighted the critical role of confinement in the behavior of concrete sections, whether circular or rectangular. Recent research by Lu et al. (2019) and Paultre & Légeron (2008) has expanded on previous findings, exploring the effects of confinement in both rectangular and circular sections. Further experimental analyses on small-scale specimens have been advanced by researchers such as Canbolat et al. (2005) and Li et al. (2023), providing further insight into material behaviors under various loading conditions. These studies continue to highlight the critical influence of steel reinforcement on the mechanical properties of concrete.

For confined concrete, Kent & Park (1971) proposed a model based on previous experimental studies. Park et al. (1982), Saatcioglu & Razvi (1992), Sheikh & Uzumeri (1982), Ahmad & Shah (1982), Mander et al. (1988), Tang et al. (2021) and Chung et al. (2002) have proposed stress-strain relationships based on the results of tests they carried out. Mander et al. (1988) propose a single mathematical relationship that describes the entire application domain. Yalcin & Saatcioglu (2000) and Hoshikuma et al. (1997) propose two behavior branches.

Each of the authors proposes stress-strain relationships that take confinement into account. Each model is more or less limited; the percentages of longitudinal ρ_l and transverse ρ_t steel are more or less restricted. The proposed relationships are applied for confinement percentages (which depend on the density of longitudinal and transversal steels) of between 20 and 25 ‰ only. When applying these models, there is a considerable discrepancy between experimental results and calculation, especially in the post-peak branch, for confinement percentages below 20 ‰. It can be noted that the ascending part is more or less representative of all these models, but the descending part after the deformation peak differs significantly from the experimental results. Another approach, carried out by Bouafia et al (Bouafia et al, 2014; Iddir, 2016) consists of the proposal of three relations to better approximate the post-peak behavior. The correlation of the stress-strain curves with the experimental results is satisfying for confinement percentages between 10 and 25 ‰.

The present work then asks how to estimate this contribution regarding the structures' ductility, particularly by considering confinement at the nodal zones at the connection of the reinforced concrete columns-beams. This study aims to model structures in reinforced concrete under monotonic increasing loads until rupture by the finite element method. The

modeling is performed considering the six degrees of freedom; it is a three-dimensional analysis.

This modeling considers the material non-linearity; the behavior relationships of concrete and steel are those derived from actual behavior until rupture. This modeling considers the geometric non-linearity and the evolution of the shear stresses due to the variation of the shear force outside the linear domain. The last parameter is considered by estimating the degradation of the shear modulus of concrete. The most interesting methods for predicting total displacements were developed from the 1980s onwards. Studies by Vecchio & Collins in 1986 (Vecchio & Collins, 1986; Kachi, 2006; Kachi et al, 2006; Houde, 2007) led to the modified compression field theory, which allows shear force to be taken into account in reinforced concrete beams. This model uses the method of strips and ties, representing a beam section by a succession of diagonal cracks crossed by transverse reinforcement.

Based on the modified compression field theory, a theoretical model presented by (Kachi, 2006) analyzes the failure behavior of reinforced and prestressed concrete beams subjected to the combined effect of plane bending and shear force in non-linear elasticity. It can be used to estimate the shear stiffness of beams with various cross-sectional shapes and reinforcement details.

The compressive strength of the concrete is limited by the strength of the concrete at the struts, which decreases as a function of the principal tensile strains perpendicular to the cracking. Cracks affect the transfer of shear forces, increasing the compressive forces to maintain equilibrium, which reduces the principal compressive stress in the concrete parallel to the cracks.

The third method used in the present study to account for the effect of shear stress is that proposed by Adjrad, which adjusts the shear modulus as a function of distortion evolution (Adjrad, 2015).

The present study is organized as follows: first, the behavior of concrete and steel used is presented, followed by the effect of transverse steel in concrete confinement. Finally, the numerical results, given by applying the software developed for this study, are compared and validated with the results of experimental tests published in the literature.

Material behavior

Concrete in compression and tension

The non-linear behavior until failure in compression of concrete, without taking into account confinement, is given by Sargin's relation

(Sargin, 1971). The advantage of this relationship is that the ascending and descending branches can be adjusted by the coefficients Kb and K'b, respectively, to the results of tests carried out on specimens of standard dimensions (Ø = 16 cm, h = 32 cm). The graphical representation of this relationship is given in Figure 1 and its mathematical expression is given by Eq.1.
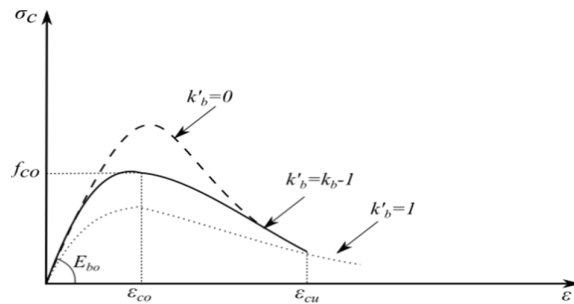

Figure 1 – Stress-strain diagram of unconfined concrete, the Sargin model

The behavior of concrete in tension is described by the relations proposed by (Grelat, 1978) and shown in Figure 2.
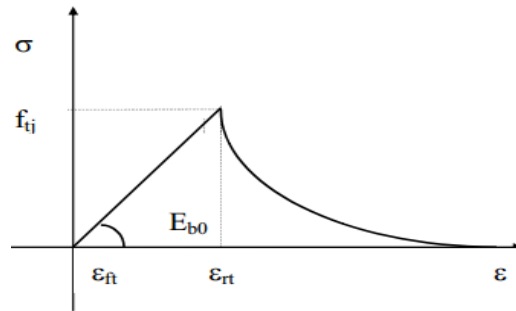

Figure 2 – Stress-strain diagram of unconfined concrete, the Grelat model

$$\sigma = f_{cj} \frac{k_b \overline{\varepsilon} - \left(k_b' - 1\right)\overline{\varepsilon}^2}{1 + \left(k_b - 1\right)\overline{\varepsilon} - k_b'\overline{\varepsilon}^2}$$

(1)

with

$$\overline{\varepsilon} = \frac{\varepsilon}{\varepsilon_0}, k_b = \frac{E_{b0}\varepsilon_0}{f_{cj}}$$

f_{cj} is the compressive strength of concrete,

1920

ε_0 is the peak deformation corresponding to f_{cj}, and

E_{b0} is the elastic modulus of concrete at the origin.

The stress-strain relationships, for the tension behavior of concrete, are given by Eq (2).

$$\sigma_{bt} = E_{b0}\varepsilon_{bt} \qquad\qquad ; |\varepsilon_{bt}| \le \varepsilon_{ft}$$

$$\sigma_{bt} = -f_{ft} \frac{(\varepsilon - \varepsilon_{rt})^2}{(\varepsilon_{rt} - \varepsilon_{ft})^2} \qquad ; \varepsilon_{ft} < |\varepsilon_{bt}| \le \varepsilon_{rt}$$

$$\sigma_{bt} = 0 \qquad\qquad ; |\varepsilon_{bt}| > \varepsilon_{rt} \qquad\qquad (2)$$

f_{tj}: is the tensile strength of concrete,

ε_{ft} is the peak deformation corresponding to f_{cj}, and

ε_{rt} is the deformation corresponding to the plasticization of the tensest steel.

Confined concrete by transverse reinforcement

The behavior of concrete confined by transverse reinforcement is described by the relations proposed by Bouafia et al. (2014). These relations define three behavior segments:
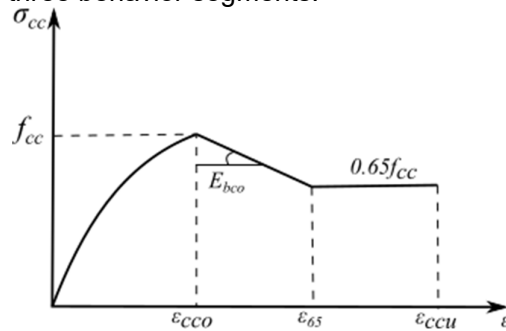

Figure 3 – Stress-strain diagram of confined concrete, model by Bouafia et al. (2014)

The first part of the curve is ascending and non-linear; the authors have proposed a modification of Sargin's relation (Sargin, 1971) to account for the confinement (see Equations 3 to 8).

For $0 \le \varepsilon_c \le \varepsilon_{cc0}$

$$\sigma_{cc} = f_{cc} \frac{k_c \bar{\varepsilon}_c - (k_c' - 1)\bar{\varepsilon}_c^2}{1 + (k_c - 2)\bar{\varepsilon}_c - k_c' \bar{\varepsilon}_c^2} \qquad\qquad (3)$$

with:

$$\overline{\varepsilon}_c = \frac{\varepsilon_c}{\varepsilon_{cc0}}$$

(4)

$$\varepsilon_{cc0} = \varepsilon_{c0}\left[1+5\left(\frac{f_{cc}}{f_{c0}}-1\right)\right]$$

(5)

$$k_c = \frac{E_{b0}\varepsilon_{cc0}}{f_{cc}}$$

(6)

$$E_{b0} = 11000\sqrt[3]{f_{cc}}$$

(7)

$$k_c^{'} = k_c - 1$$

(8)

where:

f_{cc} is the compressive strength of confined concrete,
f_{c0} is the compressive strength of unconfined concrete,
ε_{cc0} is the peak deformation corresponding to f_{cc},
ε_{c0} is the peak deformation corresponding to f_{c0}, and
K_c is the adjustment coefficient.

After reaching the maximum stress, i.e., after the peak stress, the behavior tends to decrease along a linear descending branch (this is the post-peak zone). The behavior is described by equation (9). When the longitudinal strain reaches the value given by equation (11), the stress decreases to the value given by equation (12). This stress remains constant and a ductility phase is observed, in which the deformation reaches values close to ε_{ccu} (see Equation 13).

For $\varepsilon_{cc0} \leq \varepsilon_c \leq \varepsilon_{65}$

$$\sigma_{cc} = f_{cc} - E_s\left(\varepsilon_c - \varepsilon_{cc0}\right)$$

(9)

with:

$$E_s = \frac{6f_{c0}^2}{k_e \rho_s f_{yh}}$$

(10)

$$\varepsilon_{65} = \frac{0.35f_{cc}}{E_s} + \varepsilon_{cc}$$

(11)

$$\sigma_{cc} = 0.65f_{cc}$$

(12)

$$\varepsilon_{ccu} = 0.0035 + 0.4\frac{f_l}{f_{c0}}$$

(13)

k_e is the effective confinement coefficient,
f_{yh} is the yield stress of transverse steels, and
ε_{ccu} is the ultimate strain.

1922

Behavior of steels

The behavior of steels under monotonic loads is quasi-identical in tension and compression; the steels used are natural and hardened. For natural steels, the perfect elastoplastic law is adopted (Eyrolles, 2000).

$$\sigma = E_s \varepsilon_s \qquad ; \varepsilon_s \leq \varepsilon_e$$
$$\sigma = f_e \qquad ; \varepsilon_e < \varepsilon_s < \varepsilon_u$$
$$\sigma = 0 \qquad ; \varepsilon_s > \varepsilon_u \qquad (14)$$

The behavior law of work-hardened steels is defined as follows (Eyrolles, 2000):

$$\sigma_s = E_s \varepsilon_s \qquad ; \sigma_s \leq 0.7\sigma_e$$
$$\sigma_s = \frac{\sigma_e}{E_s} + 0.823 \left(\frac{\sigma_s}{\sigma_e} - 0.7 \right)^5 \qquad ; 0.7\sigma_e < \sigma_s < 1.1\sigma_e$$
$$\sigma_s = 1.1\sigma_e \qquad ; 1\% < \varepsilon_s < \varepsilon_u \qquad (15)$$

where:
E_s is the longitudinal modulus of steel,
ε_e: is the elastic limit strain of steel,
σ_e is the elastic limit stress of steel, and
ε_u is the ultimate deformation of steel.

Degradation of the shear modulus of concrete

To more accurately predict the deformation evolution of structures subjected to increasing external forces, it is essential to take into account deformations attributed to shear in the non-linear domain. Traditional studies, such as (Kwon & Spacone, 2002; Buyukozturk, 1977), have often neglected these non-linear deformations induced by shear stress. Although shear strength can generally be estimated using simple formulas, these do not take into account the effects of bending in composite materials. In addition, the appearance of shear cracks can result in considerable shear displacement, complicating the overall response of the structure. Recent research (Lee et al, 2015; Chen et al, 2013) has addressed these complexities by incorporating shear deformations into their analysis, providing a more complete understanding of structural behavior under such conditions.

The truss analogy model, consisting of connecting diagonal concrete struts inclined at an angle θ (see Figure 4) and transverse steel ties, is

used to calculate the tensile forces in the reinforcement and the compressive forces in the concrete connecting struts subjected to longitudinal sliding forces (Bouafia, 1991).
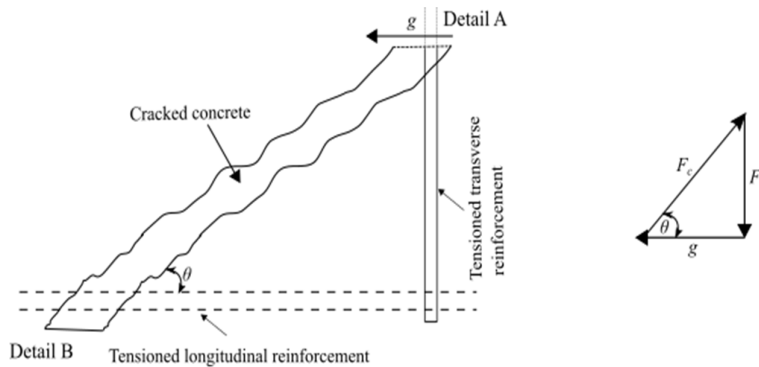

Figure 4 – Truss analogy model

The tension in the reinforcement ranges from maximum to mid-distance from the cracks (see Figure 5. A), while the strut of concrete is subjected to compression parallel to the cracks and tension in the direction of the reinforcement (see Figure 5. B). The average elongation of the reinforcement is related to the maximum stress. Modeling must take into account the compression of the concrete in the direction where the reinforcement stress is tension (Bouafia, 1991; Kachi et al, 2006).
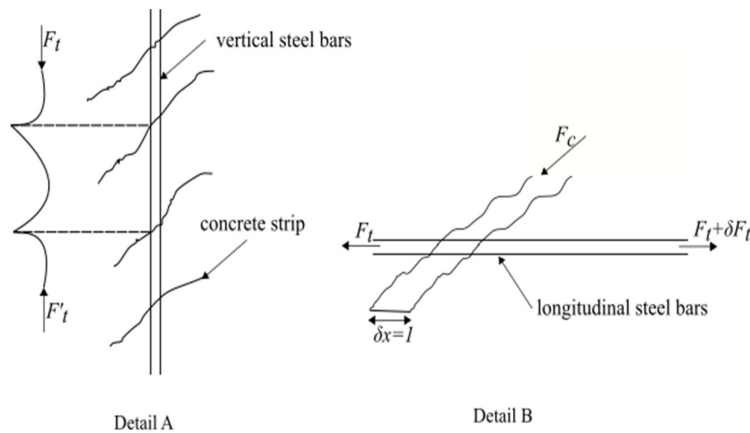

Figure 5 – Local behavior of reinforced concrete in the transverse direction (A) and the longitudinal direction (B)

In an alternative method, the degradation of the shear modulus is taken into account by applying the model proposed by (Adjrad, 2015). The authors propose expressions for estimating the value of the shear modulus as a function of the characteristics of the cross-section and the steels (see Eqs. 16, 18, 19). These expressions are given according to the three behavior zones defined in Figure 6 which allow following the degradation of this shear modulus according to the evolution of the cracking of the concrete.
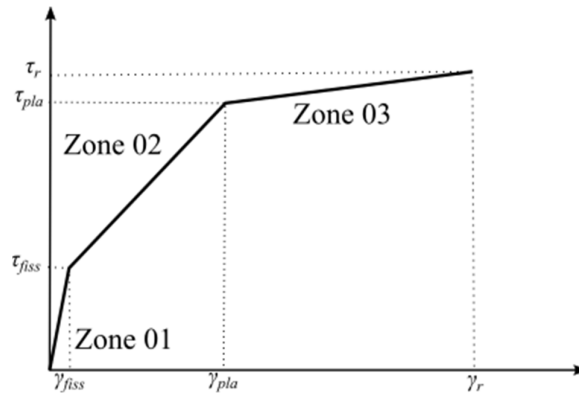

Figure 6 – Shear stress evolution versus distortion for a cross-section of reinforced concrete (Adjrad, 2015)

The model proposed by the authors is based on a theoretical and also statistical study that exploits more than 17 test results carried out on reinforced concrete beam and wall elements. These three zones are defined as follows:

Zone 01: before the concrete cracks, the variation of shear stress as a function of distortion is linear; the transverse deformation modulus G is given by the formula derived from the theory of linear elasticity (see Eq. 16).

$$G = \frac{E_c}{2(1-\mu)} \qquad for\ 0 \leq \gamma \leq \gamma_{fiss} = 0.0003$$

(16)

Zone 02: this is the post-cracking phase of the concrete and extends to the beginning of the softening of the steel. This zone is represented by a straight line whose slope is given by Eq.(17).

$$G = 604 \frac{\rho_t f_{et} \rho_l f_{el}}{f_{cj}} \qquad for\ \gamma_{fiss} \leq \gamma \leq \gamma_{plas} = 0.0025$$

(17)

Zone 03: this phase is characterized by the development of softening of the steels, and the shear modulus is given by Eq.(18).

$$G = 327 \frac{\rho_t f_{et} \rho_l f_{el}}{f_{cj}} \qquad for\ \gamma_{fiss} \leq \gamma \leq \gamma_r = 0.006$$

(18)

where:
ρ_t is the percentage of transverse reinforcement,
ρ_l is the percentage of longitudinal reinforcement,
fe_t is the yield strength of transverse reinforcement,
fe_l is the yield strength of longitudinal reinforcement,
fc_j is the characteristic compressive strength of concrete,
γ_{fiss} is the shear strain at concrete cracking,
γ_{pla} is the shear deformation due to steel plasticization,
γ_r is the shear strain at fracture, and
μ is Poisson's ratio.

The behavior of confined concrete

The compression forces applied to a reinforced concrete section produce lateral forces on the concrete inside the transverse reinforcement. The transverse steels are then solicited and thus provide concrete confinement. This (internal) confinement, generated by an adequate disposition of the steels, increases the load-bearing capacity and ductility of the structure. The compressive strength of confined concrete is given by Eq.(03) (Ngo & Scordelis, 1967; Soliman & Yu, 1967; Nait-Rabah, 1990; Spacone et al, 1992, 1996).

Circular section

The circular section, Figure 7, can be idealized by an effectively confined concrete which is inside the spiral steel, and an unconfined concrete which represents the cover.

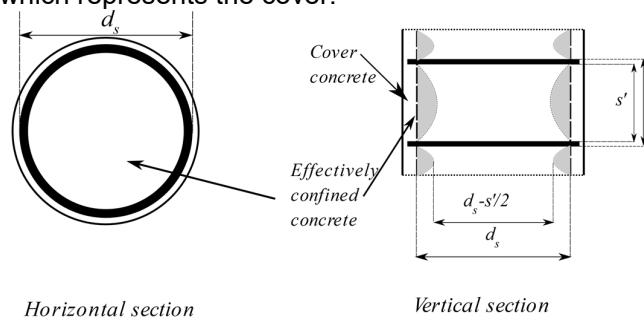*Horizontal section*　　　　*Vertical section*

Figure 7 – Confined concrete in a circular section

The confinement coefficient is defined by (Mander et al, 1988):

$$k_e = \frac{A_e}{A_{cc}} = \frac{\left(1 - \frac{s'}{2d_c}\right)}{1 - \rho_{cc}}$$

(19)

The equilibrium of forces in the section can be written as follows:

$$2 f_{yh}.A_{sp} = f_{yh}.s.d$$

(20)

The lateral confinement stress is given by:

$$f_l' = \frac{1}{2}\rho_s k_e f_{yh}$$

(21)

Rectangular section

For a rectangular section, the effective confined section is the area obtained after subtracting all the unconfined parabolas, see Figure 8. The effective confinement coefficient is given by:
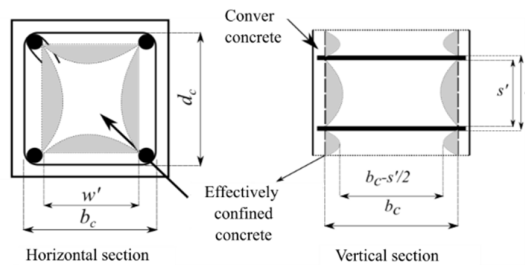

Figure 8 – Confined concrete in a rectangular section

The effective confinement coefficient is given by:

$$k_e = \frac{A_e}{A_{cc}} = \frac{\left(1 - \sum_{i=1}^{n}\frac{w_i'^2}{6b_c d_c}\right) \cdot \left(1 - \frac{s'}{2b_c}\right) \cdot \left(1 - \frac{s'}{2d_c}\right)}{(1 - \rho_{cc})}$$

(22)

1927

The longitudinal and transverse steel proportions, respectively, can be expressed by the following relationships:

$$f_{lx} = \frac{A_{sx}}{s.d_c} f_{yh} = \rho_x f_{yh}$$

(23)

$$f_{ly} = \frac{A_{sy}}{s.b_c} f_{yh} = \rho_y f_{yh}$$

(24)

The result will be:

$$f'_{lx} = k_e \rho_x f_{yh}$$

(25)

$$f'_{ly} = k_e \rho_y f_{yh}$$

(26)

The distribution of the lateral confining stress is at an angle of 45°, and the value is given by:

$$f'_l = \frac{f'_{lx} + f'_{ly}}{2}$$

(27)

Model validation

A finite element analysis software for three-dimensional reinforced concrete structures, based on the displacement method, taking into account the confinement of the concrete by the transverse reinforcements, is developed in the present study and written in Fortran language. This program is then applied to isostatic, continuous beams and column-beam structures. The comparison with the experimental results is given below and is rather satisfactory.

Confinement is taken into account using the compressive strength of the concrete, the diameter and percentage of longitudinal and transverse reinforcement, and the geometry of the concrete cross-section. A comparison is made with a series of experimental tests carried out by Mander (10 tests for circular sections and 13 tests for rectangular sections). Figures 9 and 10 present a comparison of the results between the experimental and the model of Bouafia et al, for a rectangular and circular section, respectively. (Mander et al, 1988; Bouafia et al, 2014; Iddir, 2016)
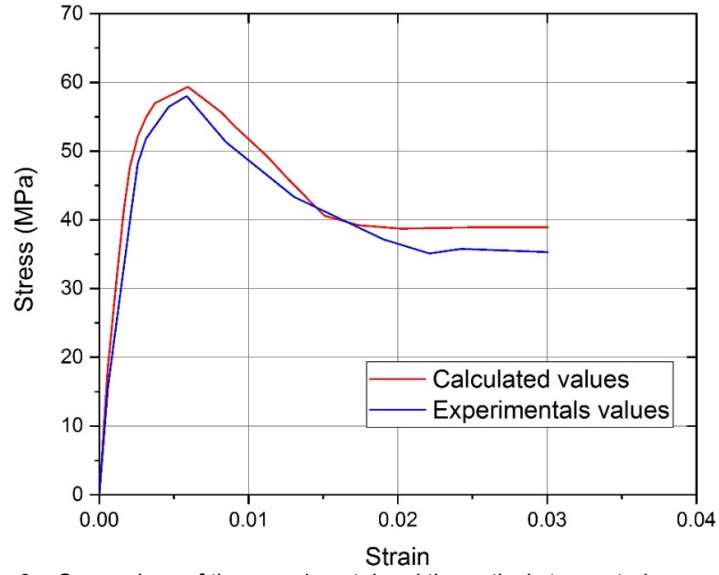
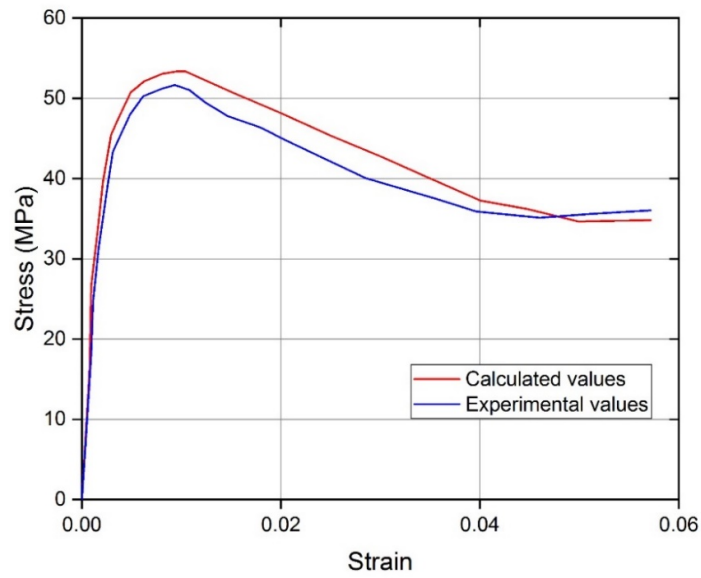*Figure 9 – Comparison of the experimental and theoretical stress-strain curves for a rectangular shape*

Figure 10 – Comparison of the experimental and theoretical stress-strain curves for circular shape

1929

The influence of taking into account the transverse reinforcement (percentage, spacing, and diameter) was demonstrated in the proposed model.

There is a clear contribution in terms of strength and ductility due to the confinement of the section. Thus, the approach adopted (proposal of three branches) provides certain flexibility to the model and therefore provides a better approach to the behavior of the material. Its application for confinement percentages from 10 to 25 ‰ is reasonably satisfactory. This model is used in the present study.

Isostatic beam: Toronto test

This experiment was done at the University of Toronto by (Vecchio & Shim, 2004). It is a program that regroups a series of tests on 12 reinforced concrete beams. In our study, we were interested in two representative beams from the geometric and reinforcement aspects: B2 and C2. The geometric characteristics are shown in Figure 11.
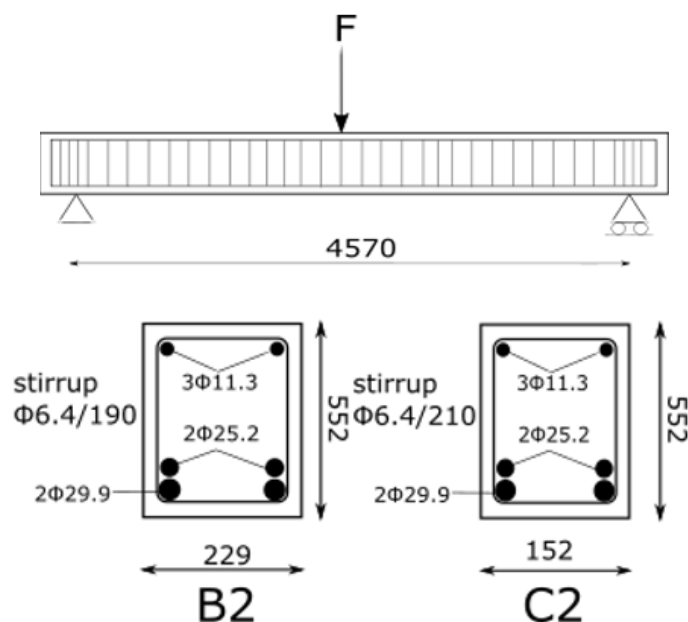

Figure 11 – Detail of the Toronto beam B2 and C2

The test consists of applying a load to the mid-span of the beam using a hydraulic jack. The load increments are 40 KN until the beam fails. The mechanical characteristics of the concrete and the longitudinal and transverse reinforcement are given in Table 1.

Table 1 – Mechanical characteristics of materials. Toronto Beam B2 and C2

Concrete	f_c' (MPa)	f_t' (MPa)	E_c (MPa)	ε_0
Beam B2	23.2	3.76	32900	0.0021
Beam C2	23.8	3.93	32900	0.0021
Steels	Diameter (mm)	Area (mm²)	f_y (MPa)	E_s (GPa)
M25	25.2	500	440	210
M30	29.9	700	436	200
Stirrup	6.4	32.2	600	200

Figures 12 and 13 show the evolution of the deflection as a function of the loading at the point of application of the incremental force. It can be seen that the simulation of our study approaches the experimental curve with good results. The concrete confinement is of course taken into account according to the real spacing of the transverse steels.

These figures show a comparison of the results with the confined concrete model used in the EN 1992-1-1 code. It can be seen that the two behavior laws for confined concrete (Bouafia et al, 2014; Eyrolles, 2000) satisfactorily approximate the actual behavior of the experimental tests on the beams B2 and C2. The experimental behavior is better approximated in the present study.
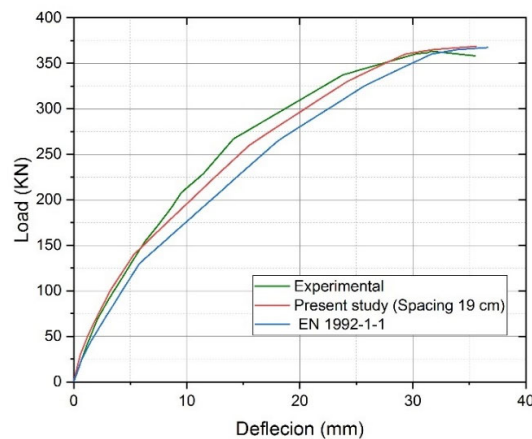

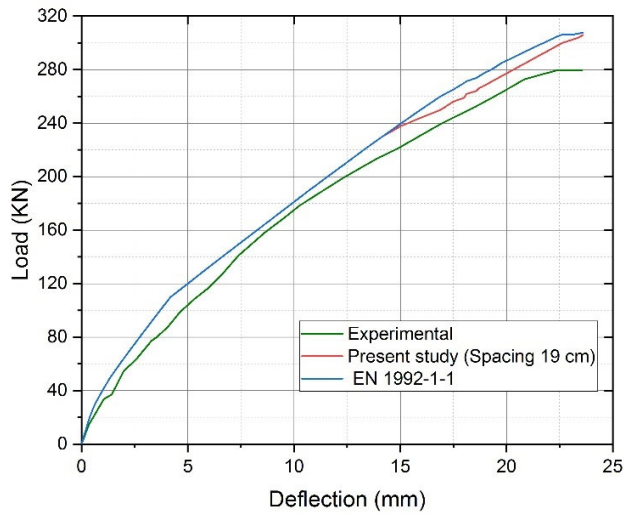*Figure 12 – Load deflection curves - Toronto Beam B2*

Figure 13 – Load deflection curves - Toronto Beam C2

Figure 14 shows the influence of transverse steel spacing on concrete confinement.
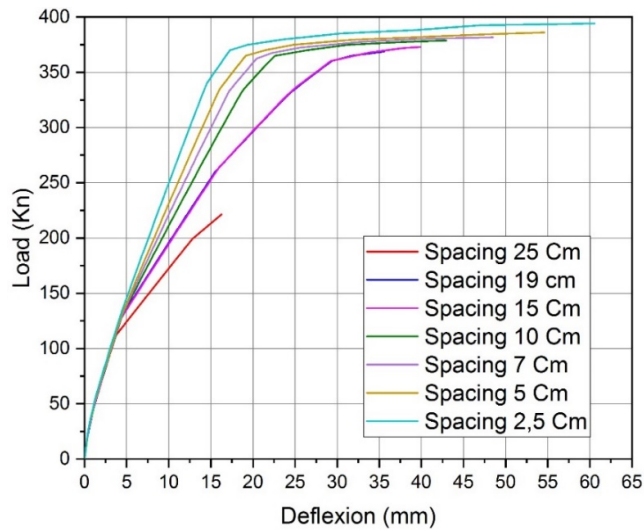

Figure 14 – Load deflection curves for different spacings – Toronto beam B2

1932

Thus, the evolution of ductility in terms of displacement, as well as a potential energy of the beam as a function of the ratio of transverse reinforcement can be observed as shown in Table 2.

Table 2 – Potential energy versus stirrup spacing. Toronto Beam B2

Spacing (cm)	Potential energy (Joules)	The gain in comparison to the experimental (%)
2.5	20479.4	124.56
5	17613.4	93.14
7	14997.1	64.45
10	14997.1	38.51
15	10680.4	17.11
25	8496.83	-83.17

Hyperstatic beam: Mattock tests

The example is taken from a series of tests carried out by Mattock (1965) on continuous hyperstatic reinforced concrete beams. The beam to be studied has two equal spans and a load point applied in the middle of the first span (see Figure 15). The cross-section beam is rectangular and the percentage of reinforcement is summarised in Table (3).

Table 3 – Mechanical characteristics of materials. Mattock beam

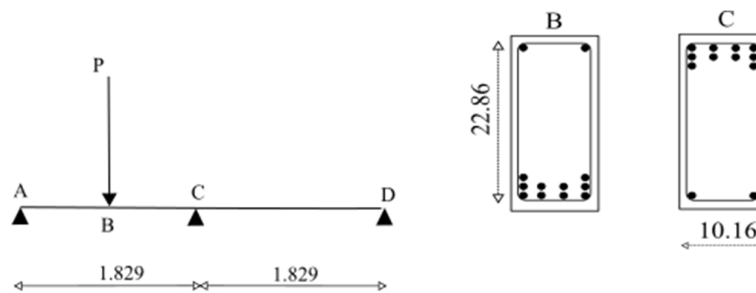| Concrete	f'_c (MPa)	f'_t (MPa)	E_c (MPa)	ε_0
Beam 03	24.99	2.1	32160	0.0024
Steels	Diameter (mm)	Area (mm²)	f_y (MPa)	E_s (GPa)
Top layer	6.35	31.67	400	200
Bottom layer	6.35	31.67	400	200
Stirrup spacing 15.24 cm	6.35	31.67	400	200

Figure 15 – Details of the Mattock beam - B3 Beam

According to Figure 16, there is a good correlation between the simulation and the experiment. The ratio between the calculated and experimental rupture load is close to 1 (see Table 4). For displacement, the relative error does not exceed 6%.
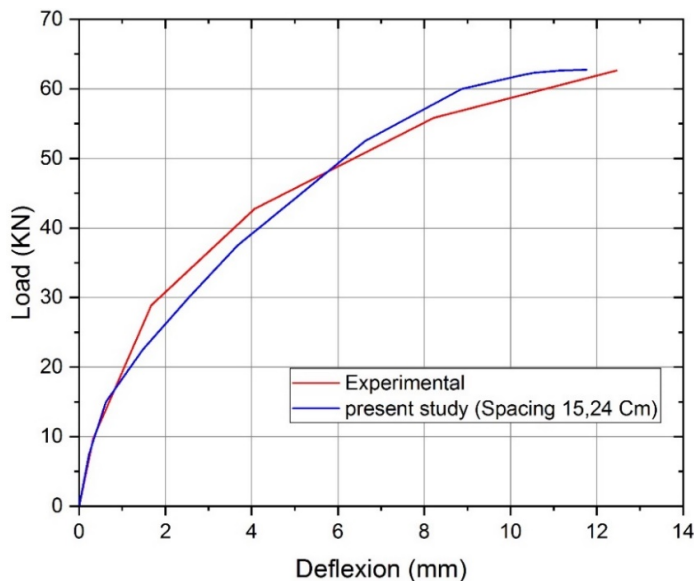

Figure 16 – Load deflection curves - Mattock beam

Table 4 – Load and displacement at the rupture. Mattock beam

	Displacement (mm)	Rupture load (KN)
Simulation	11.75	62.75
Experimental	12.45	62.63
Relative error (%)	5.62	0.19

To assess the influence of the concrete confinement, the spacing of the transverse reinforcement was increased from 2.5 to 20 cm.

The results, in terms of potential energy, gain compared to the experimental, are given in Table 5 and the behavior curves in Figure 17.

The contribution in terms of gain in potential energy and also in ductility of the beam is clearly shown.

Table 5 – Potential energy versus stirrup spacing. Mattock beam

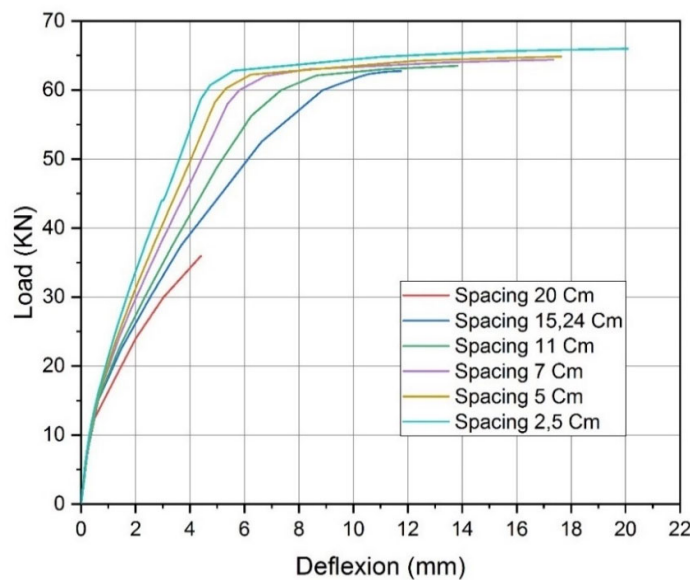| Spacing (cm)	Potential energy (Joules)	The gain in comparison to the experimental (%)
2.5	1165.13	104.77
5	976.78	71.66
7	942.30	65.60
11	685.56	20.48
20	354.43	-37.71

Figure 17 – Load deflection curves for different spacings – Mattock beam

Portal Frames: Cranston P7 - P9

The portals we are proposing for study are part of an experimental program initiated by Cranston (Grelat, 1978; Espion, 1986; Nait-Rabah, 1990; Robert, 1999).

The study concerns eight portal frames of the same dimensions, hinged at the base (Figure 18).
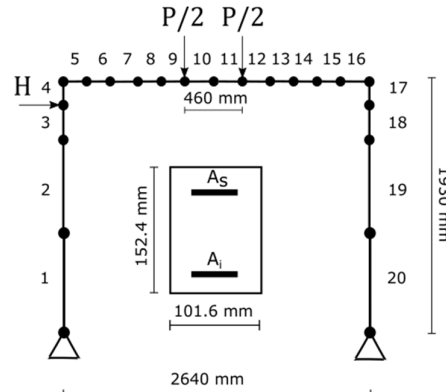
Figure 18 – Cranston portal frame

These portals are loaded at the top of the column by a force H which equals one-tenth of the force P applied at two points on the beam.
The mechanical characteristics of the portal frame are given in Table 6.

Table 6 – Mechanical characteristics of materials. Cranston portal frame

Concrete	f'_c (MPa)		f'_t (MPa)	E_c (MPa)	ε_0
Portal frame P7	33.2		2.59	32000	0.0020
Element	As ϕ 9,5	Ai ϕ 9,5	f_y (MPa)		E_s (GPa)
1, 20	2	2	278		200
2, 6, 15, 19	2	2	278		200
3, 4, 5, 16, 17, 18	2	2	278		200
7, 14	4	2	278		200
8, 13	4	2	278		200
9, 10, 11, 12	6	2	278		200

The vertical deflection at the middle section of the beam (at the junction of elements 10 and 11, see Figure 18) versus the vertical load P is shown in Figure 20.

The simulation results conform with the experimental results, especially in the linear domain and in the region of the rupture. The disparities observed in the post-cracking domain may be due to the incertitude of the mechanical properties of the steels; these are not provided by the author but are given by Grelat (1978). The difference (relative error) observed between the rupture loads (calculation/test) is 0.39% and in terms of displacement, this difference is 1.79%. (see Table 7).
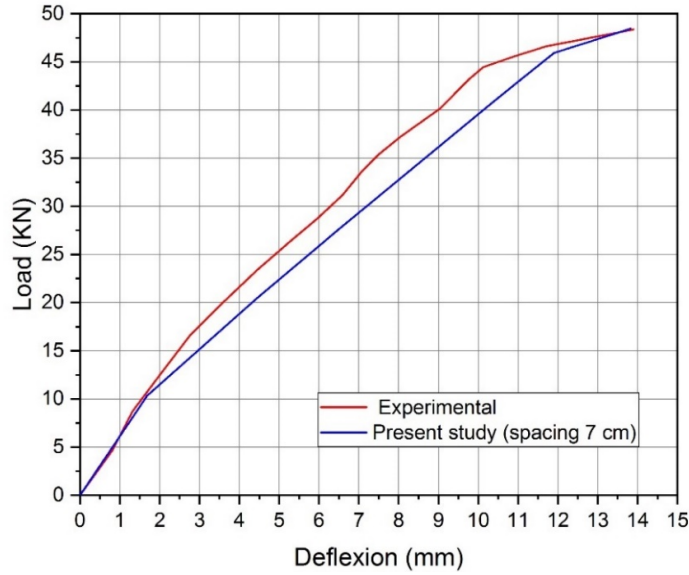
Figure - 19 Load deflection curves – Cranston portal frame

Table 7 – Load and displacement at the rupture. Cranston Portal frame

	Displacement (mm)	Rupture load (KN)
Simulation	13.64	48.16
Experimental	13.89	48.35
Relative error (%)	1.79	0.39

Closer stirrups provide a gain in potential energy. This gain is also estimated and compared to the portal frame configuration with the actual stirrup spacing (Table 8). The ductility contribution is shown in Figure 20.

Table 8 – Potential energy versus stirrup spacing. Cranston portal frame

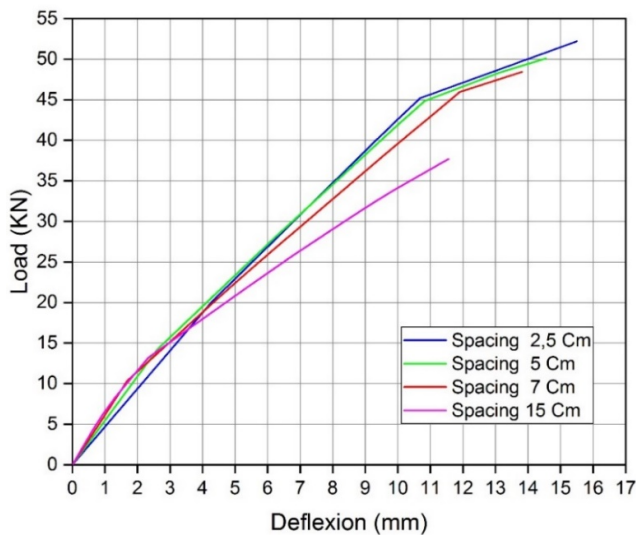| Spacing (cm)	Potential energy (Joules)	The gain in comparison to the experimental (%)
2.5	487.28	14.26
5	439.86	3.15
15	256.31	-39.90

Figure 20 – Load deflection curves for different spacings – Cranston portal frame

For the behavior of the portal frame under the effect of the horizontal load, Figure 21 shows the evolution of the horizontal displacement of the top of the portals as a function of the lateral load H.
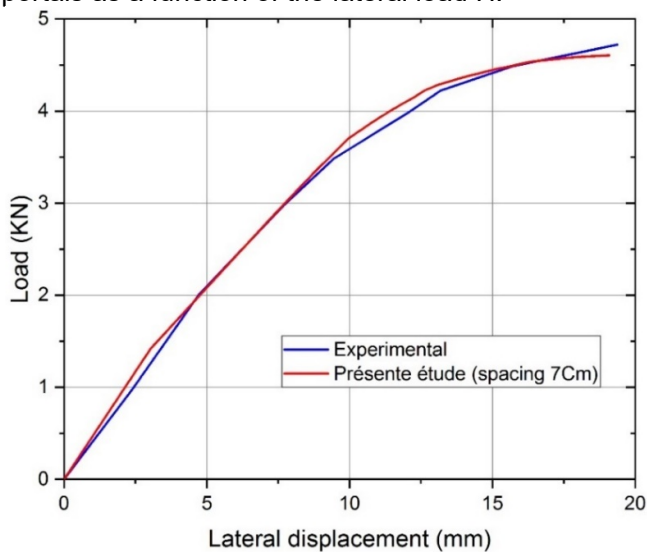

Figure 21 – Lateral displacement versus the horizontal load H – Cranston portal frame P7

The results of the calculation/test comparison are satisfactory; the behavior is well described by the numerical simulation (see Table 9).

Table 9 – Lateral load and displacement at the rupture. Cranston portal frame

	Displacement (mm)	Rupture load (KN)
Simulation	19.09	4.60
Experimental	19.37	4.63
Relative error (%)	1.46	0.60

The closer spacing of the transverse reinforcement allows better confinement of the concrete; this increases ductility (Figure 22). This gain is also reflected in an increase in potential energy, which is estimated as a function of the spacing of the transverse steels and by comparison with the experimental configuration (Table 10).

Table 10 – Potential energy versus stirrup spacing. Cranston portal frame

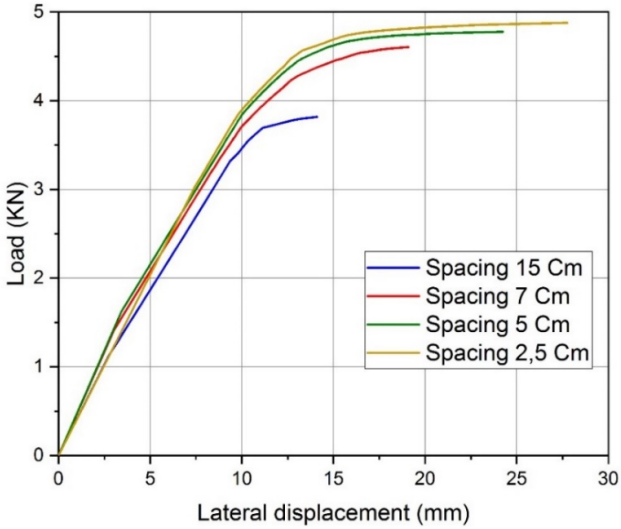| Spacing (cm)	Potential energy (Joules)	The gain in comparison to the experimental (%)
2.5	1036.49	72.84
5	860.73	43.53
15	336.47	-43.89

Figure 22 – Lateral displacement versus load for different spacings - Cranston portal frame

Conclusion

Taking into account the confinement of concrete permits us to appreciate the contribution in terms of ductility and the gain in potential energy. It also allows the increase in the ultimate load of reinforced concrete structures to be appreciated. The selected model is implemented in a computer program written in the Fortran language. This program allows following the behavior of column-beam structures subjected to variable loading until the structure's capacity is exhausted. The calculation results are compared with the experimental test results on reinforced concrete beams and frames obtained by other authors.

The comparison results, in terms of maximum load and deformability, are very satisfactory. The difference between the calculated values and those obtained experimentally does not exceed 2% in terms of maximum load. The contribution in terms of deformability represents 10 % to 70 %.

The ultimate value of the rupture load is greater the smaller the spacing of the stirrups. Finally, the influence of taking into account the confinement of concrete by transverse reinforcements on the nonlinear behavior of column-beam structures and their ductility was demonstrated.

References

Adjrad, A. 2015. *Modelisation non lineaire des structures triangulees composites*. PhD Thesis. Tizi Ouzou, People's Democratic Republic of Algeria: University Mouloud Mammeri [online]. Available at: https://dspace.ummto.dz/handle/ummto/1242 [Accessed: 28 May 2024].

Ahmad, S.H. & Shah, S.P. 1982. Complete Triaxial Stress-Strain Curves for Concrete. *Journal of the Structural Division*, 108(4), pp.728-742. Available at: https://doi.org/10.1061/JSDEAG.0005921.

Bathe, K-J. 2006. *Finite Element Procedures*. New Jersey: Prentice-Hall. ISBN: 978-0-9790049-0-2.

Bentz, E.C. & Collins, M.P. 2000. *Response-2000: Load-Deformation Response of Reinforced Concrete Sections* [online]. Available at: https://ingenieriasismica.utpl.edu.ec/sites/default/files/publicaciones/UCG-ES-00012.pdf [Accessed: 28 May 2024].

Blume, J.A., Newmark, N.M. & Corning, L.H. 1961. *Design of multistory reinforced concrete buildings for earthquake motions.* Portland Cement Association.

Bouafia, Y. 1991. *Résistance à l'effort tranchant des poutres en béton à precontrainte exterieure : étude experimentale et calcul à la rupture.* PhD Thesis. Châtenay-Malabry, Ecole centrale de Paris [online]. Available at: http://www.theses.fr/1991ECAP0198 [Accessed: 28 May 2024].

Bouafia, Y., Iddir, A., Kachi, M.S. & Dumontet, H. 2014. Stress-Strain relationship for the confined concrete. In: *11th World Congress on Computational Mechanics (WCCM XI)*, Barcelona, Spain, July 20 - 25 [online]. Available at: https://congress.cimne.com/iacm-eccomas2014/admin/files/fileabstract/a1410.pdf [Accessed: 28 May 2024].

Bratina, S., Saje, M. & Planinc, I. 2004. On materially and geometrically non-linear analysis of reinforced concrete planar frames. *International Journal of Solids and Structures*, 41(24-25), pp.7181-7207. Available at: https://doi.org/10.1016/j.ijsolstr.2004.06.004.

Buyukozturk, O. 1977. Nonlinear analysis of reinforced concrete structures. *Computers & Structures*, 7(1), pp.149-156. Available at: https://doi.org/10.1016/0045-7949(77)90069-4.

Canbolat, B.A., Parra-Montesinos, G.J. & Wight, J.K. 2005. Experimental Study on Seismic Behavior of High-Performance Fiber-Reinforced Cement Composite Coupling Beams. *ACI Structural Journal*, 102(1), pp.159-166. Available at: https://doi.org/10.14359/13541.

Chen, G., Teng, J.G. & Chen, J.-F. 2013. Shear Strength Model for FRP-Strengthened RC Beams with Adverse FRP-Steel Interaction. *Journal of Composites for Construction*, 17(1), pp.50-66. Available at: https://doi.org/10.1061/(ASCE)CC.1943-5614.0000313.

Chung, H.-S., Yang, K.-H., Lee, Y.-H. & Eun, H.-C. 2002. Stress–strain curve of laterally confined concrete. *Engineering structures*, 24(9), pp.1153-1163. Available at: https://doi.org/10.1016/S0141-0296(02)00049-4.

Eltoft, T. & Lande, T. 2015. *Nonlinear Analyses of RC Frames under Vertical and Horizontal Loading*. Master's Thesis. Trondheim, Torgarden, Norway: Norwegian University of Science and Technology - NTNU [online]. Available at: https://hdl.handle.net/11250/2351358 [Accessed: 28 May 2024].

Elwood, K.J. & Moehle, J.P. 2003. *Shake Table Tests and Analytical Studies on the Gravity Load Collapse of Reinforced Concrete Frames*. Pacific Earthquake Engineering Research Center, College of Engineering, University of California, Berkeley [online]. Available at: https://peer.berkeley.edu/sites/default/files/0301_k._elwood_j._moehle.pdf [Accessed: 28 May 2024].

Espion, B. 1986. *Contribution à l'analyse non linéaire des ossatures planes. Application aux structures en béton armé*. PhD Thesis. Bruxelles: Université libre de Bruxelles, Faculté des sciences [online]. Available at: https://difusion.ulb.ac.be/vufind/Record/ULB-DIPOT:oai:dipot.ulb.ac.be:2013/213542/Details [Accessed: 28 May 2024].

-Eyrolles. 2000. *Regles Bael 91 Modifiees 99. 3eme Edition: Règles techniques de conception et de calcul des ouvrages et constructions en béton armé suivant la méthode des états-limites*. Eyrolles. ISBN: 978-2212100235.

Grelat, A. 1978. *Calcul non linéaire des ossatures en béton armé*. PhD Thesis. Paris 6: Pierre and Marie Curie University - UPMC.

Hoshikuma, J., Kawashima, K., Nagaya, K. & Taylor, A.W. 1997. Stress-Strain Model for Confined Reinforced Concrete in Bridge Piers. *Journal of*

Structural Engineering, 123(5), pp.624-633. Available at: https://doi.org/10.1061/(ASCE)0733-9445(1997)123:5(624).

Houde, M.-J. 2007. *Modélisation de poutres en béton armé endommagées par chargements cycliques: comportement en flexion et en cisaillement*. PhD Thesis. Québec, Canada: Université Laval, Faculty of Civil Science and Engineering, Department of Engineering [online]. Available at: https://library-archives.canada.ca/eng/services/services-libraries/theses/Pages/item.aspx?idNumber=1276807867 [Accessed: 28 May 2024].

Iddir, A. 2016. *Modélisation des éléments de structure de section circulaire en béton armé confiné (Analyse de la fissuration)*. PhD Thesis. Tizi-Ouzou, Algeria: University Mouloud Mammeri, Faculty of Engineering and Construction, Department of Civil Engineering [online]. Available at: https://dspace.ummto.dz/server/api/core/bitstreams/0b664013-a868-4a03-9a0b-d50ad7b5b523/content [Accessed: 28 May 2024].

Kachi, M.S. 2006. *Modélisation du comportement jusqu'à rupture des poutres à précontrainte extérieure*. PhD Thesis. Tizi-Ouzou, Algeria: University Mouloud Mammeri, Faculty of Engineering and Construction, Department of Civil Engineering.

Kachi, M.S., Fouré, B., Bouafia, Y. & Muller, P. 2006. L'effort tranchant dans la modélisation du comportement jusqu'à rupture des poutres en béton armé et précontraint. *Revue Européenne de Génie Civil*, 10(10), pp.1235-1264. Available at: https://doi.org/10.1080/17747120.2006.9692914.

Kent, D.C. & Park, R. 1971. Flexural Members with Confined Concrete. *Journal of the Structural Division*, 97(7), pp.1969-1990. Available at: https://doi.org/10.1061/JSDEAG.0002957.

Kwon, M. & Spacone, E. 2002. Three-dimensional finite element analyses of reinforced concrete columns. *Computers & Structures*, 80(2), pp.199-212. Available at: https://doi.org/10.1016/S0045-7949(01)00155-9.

Lee, J.-Y., Lee, D.H., Lee, J.-E. & Choi, S.-H. 2015. Shear Behavior and Diagonal Crack Width for Reinforced Concrete Beams with High-Strength Shear Reinforcement. *ACI Structural Journal*, 112(3), pp.323-334. Available at: https://doi.org/10.14359/51687422.

Li, H., Li, X., Fu, J., Zhu, N., Chen, D., Wang, Y. & Ding, S. 2023. Experimental study on compressive behavior and failure characteristics of imitation steel fiber concrete under uniaxial load. *Construction and Building Materials*, 399, art.number:132599. Available at: https://doi.org/10.1016/j.conbuildmat.2023.132599.

Lu, Y., Liu, Z., Li, S. & Zhao, X. 2019. Effect of the Outer Diameter on the Behavior of Square RC Columns Strengthened with Self-Compacting Concrete Filled Circular Steel Tube. *International Journal of Steel Structures*, 19, pp.1042-1054.

Mander, J.B., Priestley, M.J.N. & Park, R. 1988. Theoretical Stress-Strain Model for Confined Concrete. *Journal of Structural Engineering*, 114(8), pp.1804-1826. Available at: https://doi.org/10.1061/(ASCE)0733-9445(1988)114:8(1804).

Mattock, A.H. 1965. Rotational Capacity of Hinging Regions in Reinforced Concrete Beams, Flexural Mechanics of Reinforced Concrete. In: *Proceedings of the ASCE-ACI Internatl. Symposium,* Miami, Fl, USA, 12, pp.143-181, November 10-12 [online]. Available at: https://www.concrete.org/publications/internationalconcreteabstractsportal.aspx?m=details&id=16716 [Accessed: 28 May 2024].

Nait-Rabah, O. 1990. *Simulation numérique du comportement non-linéaire des ossatures spatiales*. PhD Thesis. Châtenay-Malabry, Ecole centrale de Paris [online]. Available at: https://theses.fr/1990ECAP0151 [Accessed: 28 May 2024].

Ngo, D. & Scordelis, A.C. 1967. Finite Element Analysis of Reinforced Concrete Beams. *ACI Journal Proceedings*, 64(3), pp.152-163. Available at: https://doi.org/10.14359/7551.

Park, R., Priestley, M.J.N. & Gill, W.D. 1982. Ductility of Square-Confined Concrete Columns. *Journal of the Structural Division*, 108(4), pp.929-950. Available at: https://doi.org/10.1061/JSDEAG.0005933.

Paultre, P. & Legeron, F. 2008. Confinement Reinforcement Design for Reinforced Concrete Columns. *Journal of Structural Engineering*, 134(5). Available at: https://doi.org/10.1061/(ASCE)0733-9445(2008)134:5(738).

Popovics, S. 1973. A numerical approach to the complete stress-strain curve of concrete. *Cement and concrete research*, 3(5), pp.583-599. Available at: https://doi.org/10.1016/0008-8846(73)90096-3.

Robert, F. 1999. *Contribution à l'analyse non linéaire géométrique et matérielle des ossatures spatiales en Génie Civil : application aux ouvrages d'art*. PhD thesis. Lyon, France: INSA - National Institute of Applied Sciences [online]. Available at: https://theses.fr/1999ISAL0032 [Accessed: 28 May 2024].

Roy, H.E.H. & Sozen, M.A. 1965. Ductility of Concrete. *ACI Symposium Publication*, 12, pp.213-235 [online]. Available at: https://www.concrete.org/publications/internationalconcreteabstractsportal/m/details/id/16718 [Accessed: 28 May 2024].

Rozman, M. & Fajfar, P. 2009. Seismic response of a RC frame building designed according to old and modern practices. *Bulletin of Earthquake Engineering,* 7(3), pp.779-799. Available at: https://doi.org/10.1007/s10518-009-9119-4.

Saatcioglu, M. & Razvi, S.R. 1992. Strength and Ductility of Confined Concrete. *Journal of Structural engineering*, 118(6), pp.1590-1607. Available at: https://doi.org/10.1061/(ASCE)0733-9445(1992)118:6(1590).

Sargin, M. 1971. *Stress-strain Relationships for Concrete and the Analysis of Structural Concrete Sections*. Waterloo, Ont: University of Waterloo, Solid Mechanics Division.

Scott, B.D., Park, R. & Priestley, M.J.N. 1982. Stress-Strain Behavior of Concrete Confined by Overlapping Hoops at Low and High Strain Rates. *ACI Journal Proceedings*, 79(1), pp.13-27. Available at: https://doi.org/10.14359/10875.

Sheikh, S.A. & Uzumeri, S.M. 1982. Analytical Model for Concrete Confinement in Tied Columns. *Journal of the Structural Division*, 108(12), pp.2703-2722. Available at: https://doi.org/10.1061/JSDEAG.0006100.

Soliman, M.T.M. & Yu, C.W. 1967. The flexural stress-strain relationship of concrete confined by rectangular transverse reinforcement. *Magazine of Concrete Research*, 19(61), pp.223-238. Available at: https://doi.org/10.1680/macr.1967.19.61.223.

Spacone, E., Ciampi, V. & Filippou, F.C. 1992. *Beam Element for Seismic Damage Analysis*. Berkeley: University of California, College of Engineering, Earthquake Engineering Research Center, Report No. UCB/EERC-92/07 [online]. Available at: https://nehrpsearch.nist.gov/article/PB95-192126/XAB [Accessed: 28 May 2024].

Spacone, E., Filippou, F.C. & Taucer, F.F. 1996. Fibre beam–column model for non-linear analysis of R/C frames: Part I. Formulation. *Earthquake Engineering & Structural Dynamics*, 25(7), pp.711-725. Available at: https://doi.org/10.1002/(SICI)1096-9845(199607)25:7<711::AID-EQE576>3.0.CO;2-9.

Tang, H., Liu, R., Zhao, X., Guo, R. & Jia, Y. 2021. Axial compression behavior of CFRP-confined rectangular concrete-filled stainless steel tube stub column. *Frontiers of Structural and Civil Engineering*, 15, pp.1144-1159. Available at: https://doi.org/10.1007/s11709-021-0762-4.

Vecchio, F.J. & Collins, M.P. 1986. The Modified Compression-Field Theory for Reinforced Concrete Elements Subjected to Shear. *ACI Journal Proceedings*, 83(2), pp.219-231. Available at: https://doi.org/10.14359/10416.

Vecchio, F.J. & Shim, W. 2004. Experimental and Analytical Reexamination of Classic Concrete Beam Tests. *Journal of Structural Engineering*, 130(3), pp.460-469. Available at: https://doi.org/10.1061/(ASCE)0733-9445(2004)130:3(460).

Yalcin, C. & Saatcioglu, M. 2000. Inelastic analysis of reinforced concrete columns. *Computers & Structures*, 77(5), pp.539-555. Available at: https://doi.org/10.1016/S0045-7949(99)00228-X.

Zienkiewicz, O.C. & Taylor, R.L. 2005. *The Finite Element Method for Solid and Structural Mechanics, 6th Edition*. Butterworth-Heinemann. ISBN: 9780750663212.

Influencia del confinamiento por refuerzo transversal sobre el comportamiento no lineal de estructuras de hormigón armado

Adnane Ourabah, **autor de correspondencia**, *Youcef* Bouafia, *Abdelkader* Iddir, *Mohand Said* Kachi

Universidad Mouloud Mammeri, Departamento de Ingeniería Civil, Laboratorio L2MSGC,
Tizi Ouzou, República Argelina Democrática y Popular

CAMPO: ingeniería mecánica, ingeniería civil
TIPO DE ARTÍCULO: artículo científico original

Resumen:

Introducción/objetivo: El diseño y cálculo estructural se basan en el comportamiento del hormigón y del acero por separado, sin tener en cuenta el aporte de los estribos en el confinamiento del hormigón. La influencia del confinamiento en el modelado estructural se puede utilizar para aproximarse mejor al comportamiento real. El propósito de este estudio es desarrollar y validar un modelo no lineal para el comportamiento de estructuras de hormigón armado, teniendo en cuenta el confinamiento del hormigón.

Métodos: Se utiliza un modelo de elementos finitos 3D para analizar estructuras enmarcadas. Este modelo tiene en cuenta las deformaciones por corte. La sección transversal de la viga se discretiza en capas trapezoidales, mientras que se supone que cada capa está estresada uniaxialmente. A los materiales se les aplican leyes constitutivas no lineales. Para el confinamiento del hormigón, la ductilidad del material se considera utilizando las relaciones propuestas por Bouafia et al. Estos modelos se implementan en un programa informático. El software monitorea el comportamiento de estructuras columna-viga bajo cargas variables hasta alcanzar su capacidad portante.

Resultados: Los resultados se comparan con los resultados del experimento, centrándose en la máxima resistencia y deformabilidad. La comparación muestra resultados muy satisfactorios. Además, el uso de refuerzo transversal para el confinamiento del hormigón impacta significativamente el comportamiento global de las estructuras de hormigón armado al influir en la contribución de la ductilidad.

Conclusión: La consideración del confinamiento en estructuras proporciona la mejor aproximación posible al comportamiento real de las estructuras. A diferencia de los códigos de cálculo existentes, las leyes de comportamiento del hormigón no tienen en cuenta la contribución del confinamiento mediante el refuerzo transversal.

Palabras claves: refuerzo, confinamiento, modelado, simulación, ductilidad, estribos.

Влияние давления поперечной арматуры на нелинейные характеристики железобетонных конструкций

Аднан Ораба, **корреспондент**, *Jусуф* Буафиа,
Абделкадер Иддир*, Муханд Саид* Качи

Университет Мулауд Маммери,
Факультет гражданского строительства, лаборатория L2MSGC,
г. Тизи-Узу, Алжирская Народная Демократическая Республика

Резюме:

Введение/цель: Проектирование и расчет конструкций основаны на поведении бетона и стали, рассматриваемых отдельно, без учета влияния хомутов в предварительно напряженном бетоне. Эффект давления при структурном моделировании можно использовать для лучшего приближения к реальному поведению. Целью данного исследования является разработка и испытание нелинейной модели поведения железобетонных конструкций с учетом сжатия бетона.

Методы: Для расчета железобетонных конструкций используется трехмерная модель конечных элементов, учитывающая сдвиговые деформации. Поперечное сечение балки разделено на трапециевидные слои, при этом предполагается, что каждый слой имеет одноосное напряжение. К материалам применяются нелинейные определяющие законы. Для определения прочности бетона учитывается пластичность материала с использованием соотношений, предложенных Буафией и соавторами. Эти модели реализованы в компьютерной программе. Программное обеспечение отслеживает поведение колонно-балочных конструкций при переменных нагрузках до достижения их несущей способности.

Результаты: Полученные результаты сравнивались с результатами экспериментов с акцентом на максимальную прочность и деформируемость. Сравнительный анализ показал весьма удовлетворительные результаты. Помимо того, использование поперечного армирования для прочности бетона существенно влияет на общие характеристики железобетонных конструкций, в том числе и на его пластичность.

Вывод: Учет сжатия в конструкциях обеспечивает наилучший подход к реальному поведению конструкций. В отличие от существующих правил расчета, законы поведения бетона не учитывают влияние сжатия за счет поперечного армирования.

Ключевые слова: армирование, сжатие, моделирование, симуляция, пластичность, хомуты.

Утицај притискања попречном арматуром на нелинеарно понашање   армиранобетонских конструкција

Аднан Ораба, **аутор за преписку**, *Јусуф* Буафиа,
Абделкадер Идир, *Муханд Саид* Качи

Универзитет „Мулуд Мамери",
Одељење за грађевинарство, Лабораторија L2MSGC,
Тизи Узу, Народна Демократска Република Алжир

ОБЛАСТ: машинство, грађевинарство
КАТЕГОРИЈА (ТИП) ЧЛАНКА: оригинални научни рад

Сажетак:

Увод/циљ: Пројектовање и прорачун конструкција заснивају се на понашању бетона и челика посматраних одвојено, без узимања у обзир утицаја узенгија у притиснутом бетону. Утицај притискања у моделовању конструкције може се искористити за бољу апроксимацију стварног понашања. У студији је развијен и тестиран нелинеарни модел за понашање армиранобетонских конструкција, узимајући у обзир притискање бетона.

Методе: За анализу армираних конструкција користи се модел коначних елемената 3Д који узима у обзир деформације смицања. Попречни пресек греде је дискретизован у слојеве облика трапеза где се за сваки слој узима де је у једноосном стању напрезања. Примењују се нелинеарни конститутивни закони материјала. За притискање бетона разматра се дуктилност материјала коришћењем релација предложених у Буафиа и др. Ти модели су имплементирани у компјутерски програм. Софтвер прати понашање конструкција стуб-греда под различитим оптерећењима до достизања њихове пуне носивости.

Резултати: Резултати који су поређени са експерименталним резултатима, нарочито када је реч о максималној чврстоћи и деформабилности, показали су се као веома задовољавајући. Поред тога, коришћење попречног ојачања за притискање бетона утиче на понашање армиранобетонских конструкција у целини путем доприноса дуктилности.

Закључак: Разматрање притиснутости у конструкцијама обезбеђује најбољи могући приступ понашању конструкција у реалности. За разлику од постојећих прорачунских израза, закони понашања бетона не узимају у обзир допринос притискања помоћу попречне арматуре.

Кључне речи: армирање, притискање, моделовање, симулација, дуктилност, узенгије.